DOI: 10.1002/adma.200601338

Construction of Chiral Propeller Architectures from Achiral Molecules**

By *Kwang-Un Jeong*, *Deng-Ke Yang*, *Matthew J. Graham*, *Yingfeng Tu*, *Shiao-Wei Kuo*, *Brian S. Knapp*, *Frank W. Harris*, and *Stephen Z. D. Cheng**

Of particular interest to the next generation of biological and electro-optical advances in materials science and technology is the recognition and translation of chirality to different length scales in self-assembled systems.[1–7] Understanding and controlling this is essential for mimicking the development of biological structures and for achieving tailored macroscopic properties.[8–17] Classically, chirality is generated by the incorporation of asymmetric tetrahedral carbons, but self-assembled liquid crystal (LC) materials formed through non-covalent interactions, such as H-bonding, have attracted much attention, as these materials may also possess chirality independent of molecular chirality. Amplification processes can enable chirality transfer from the nanometer scale to the macroscopic scale, as is often observed in Nature. Here, we show for the first time that chiral propellers can be constructed from achiral molecules (BPCA-C*n*-P*m*OH, i.e., 4-biphenylcarboxylic acid molecules connected to alkoxyl chains with varying number of carbon atoms ($n = 6$–10) and terminated with phenyl groups with hydroxyl groups at the meta-position, as shown in Fig. 1a) via H-bond-driven self-assembly.

We have previously shown that this series of achiral BPCA-C*n*-P*m*OH molecules, having neither molecular chirality[8–17] nor a significantly bent core (like banana-shaped molecules),[18–23] can form 3D helical supramolecular structures in a smectic C (SmC) phase.[24,25] These helical structures can be caused by the molecular tilting of twisted head-to-head H-bonded dimers (Fig. 1a) during the SmA to SmC phase transition.[25] The question becomes: can an achiral molecule that is not in a smectic phase construct phases with intrinsic cholesteric chiral characteristics? The answer to this question would provide significant insight into the most basic requirements needed to form chiral phases, which are critical in biology and optics.

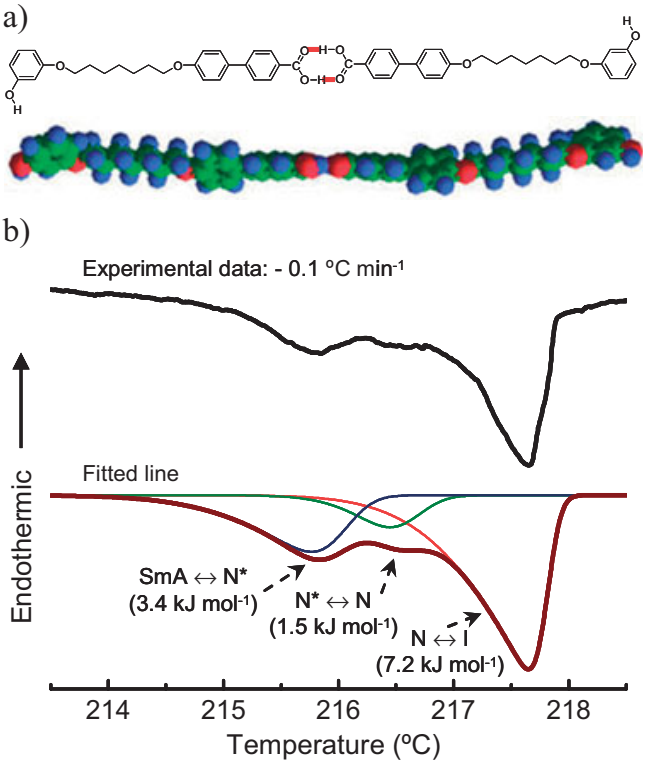

Figure 1. a) The chemical structure of the dimeric building block of BPCA-C7-P*m*OH (red line represents H-bonding) and its energy-minimized chiral conformation. b) The differential scanning calorimetry (DSC) thermal diagram (black line) at a cooling rate of 0.1 °C min^{-1} and its analytical deconvolution (maroon line) of three transitions: SmA–N* (navy blue), N*-N (olive green) and N-I (red) transitions.

The differential scanning calorimetry (DSC) of BPCA-C7-P*m*OH at a slow cooling rate (0.1 °C min^{-1}) is shown in Figure 1b. Through the analytical deconvolution of the experimentally observed exothermic processes we deduced one exothermic transition at 216.5 °C (with a heat of transition of 1.5 kJ mol^{-1}) between the achiral nematic (N) phase and the SmA phase. However, identifying the structural characteristics of this phase required other experimental methods.

First, the BPCA-C*n*-P*m*OH molecules were placed in between two polyimide-coated/rubbed (antiparallel) substrates (the detailed preparation procedure of the substrates can be found in the literature[26]). Polyimide-coated substrates are hydrophobic (with a contact angle of 82° ± 5°), so they prefer interacting with aromatic rings.[27] Rubbed polyimide layers

[*] Prof. S. Z. D. Cheng, Dr. K.-U. Jeong, Dr. M. J. Graham, Dr. Y. Tu, Dr. S.-W. Kuo, Dr. B. S. Knapp, Prof. F. W. Harris
Maurice Morton Institute and Department of Polymer Science
The University of Akron
Akron, OH 44325 (USA)
E-mail: scheng@uakron.edu
Prof. D.-K. Yang
Liquid Crystal Institute, Kent State University
Kent, OH 44242 (USA)

[**] This work was supported by the National Science Foundation of USA (DMR-0516602) and the Collaborative Center in Polymer Photonics between the Air Force Research Laboratory Materials and Manufacturing Directorate and The University of Akron.

ADVANCED MATERIALS

can orient BPCA-C*n*-P*m*OH dimers and generate larger LC monodomains. The changes in the optical textures of BPCA-C7-P*m*OH were investigated with polarized optical microscopy (POM). Upon cooling, the transition from the isotropic melt to the achiral N phase occurred at 218 °C. Birefringent achiral N droplets appeared and grew from the isotropic background. When the temperature reached 216 °C, characteristic cholesteric helical structures similar to other chiral N systems, such as a Frank–Pryce spherulitic N droplet with equidistant rings,[2,28] (Fig. 2a) and fingerprint textures with equidistant lines,[27] (Fig. 2b) were observed. Note that in fingerprint textures there is no mechanical confinement that can create helical structures from achiral molecules.[29,30] In the case of the Frank–Pryce spherulitic N droplet and fingerprint texture, the helical axis was perpendicular to the alternating birefringent lines, and the LC molecular directors were perpendicular to and rotating around the helical axis, as illustrated in Figure 2c and d. In this case, the dimers were only undergoing a single twist perpendicular to the helical axis. The pitch length of the Frank–Pryce spherulitic N droplet and fingerprint texture was (2.5 ± 0.5) μm. The average distance between neighboring dimer layers along the helical axis in the N phase, as evaluated with wide-angle X-ray diffraction (WAXD), was 0.48 nm.[24] Therefore, about 5200 dimers are needed to construct one pitch. The calculated local twisting angle between the neighboring dimer layers was ca. 0.07°. Upon further decreasing the temperature toward the SmA phase, the equidistant lines disappeared from the center of the chiral N droplets, in a similar way to chiral molecular systems.[27]

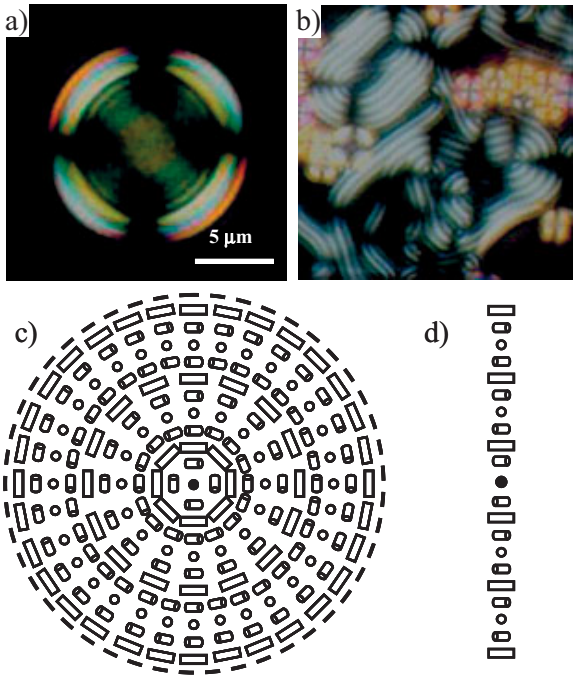

Figure 2. POM textures of BPCA-C7-P*m*OH in a polyimide-coated/rubbed glass cell: a) Frank–Pryce spherulitic N droplet and b) fingerprint textures at 216 °C. c) The molecular-packing model and d) molecular arrangement along the radial direction of the droplets.

In contrast to polyimide-coated/rubbed glass substrates, the hydrophilic surface of unrubbed bare glass substrates (contact angle of 35° ± 3°) can interact with the hydroxy groups at the end of the BPCA-C*n*-P*m*OH dimers via H-bonding.[31,32] The achiral N droplets first formed and grew, following a nucleation mechanism, against the isotropic background seen through POM. When the temperature reached 216 °C, surprisingly, a mixture of right-handed and left-handed propeller-patterned chiral N droplets (Fig. 3a) formed with the achiral N droplets. Since the sample thickness between the two glass substrates was ca. 5 μm, those propeller-patterned chiral N droplets with a diameter smaller than the sample thickness were 3D spheres or surface-attached hemispheres, while those propeller-patterned chiral N droplets with a diameter larger than the sample thickness were pancakelike. This is the first time that propeller patterns have been observed in rodlike achiral molecules.

Based on the Oseen–Frank elastic energy density,[27] a computer-calculated LC molecular-packing model of a right-handed propeller-patterned N droplet is illustrated in Figure 3c. In this model, the helical axis was considered to be along the radial direction. In a cylindrical coordinate system (θ, ϕ, z), θ is the twist angle between the z axis (cylinder axis) and the LC molecular director (n), and ϕ is the azimuthal twist angle perpendicular to the z axis. The LC molecular director is thus twisted along both the θ and ϕ twisting angles. At the center of the droplets, the LC molecular director was parallel to the z axis, and at the edge of the droplets, the LC molecular director was perpendicular to the z axis (parallel to the helical axis). Therefore, the propeller-patterned chiral N droplet was a case of double twisting, as illustrated in Figure 3c. The calculated propeller-patterned chiral N droplet texture (Fig. 3d) agrees well with the experimental observation (Fig. 3a).

The director configuration of this LC molecular model could also be confirmed by POM textures with a tint-retardation plate between the sample and the analyzer (Fig. 3b). The propeller-patterned chiral N droplets, shown in Figure 3b, had their dimers perpendicular to the edge of the droplets, which agreed with the molecular-packing model of the propeller-patterned chiral N droplet (Fig. 3c) and its calculated texture with a retardation plate (Fig. 3e). While rotating the sample between a polarizer and analyzer (at a 90° angle with respect to each other), the dark regions in the chiral propeller-patterned N droplet do not change. This indicates that C_∞ symmetry exists in the angular direction of these droplets. Furthermore, when the projections $r(\phi)$ of the molecular directors were parallel to the polarizer or the analyzer, the four circular dark regions appeared, as shown in Figure 3a and in its calculated texture (Fig. 3d).

It is worthwhile to note that the helical pitch of these chiral propeller-patterned N droplets was $2R$, where R was the radius of propeller-patterned chiral N droplet. This indicated that the helical pitch of these propeller-patterned chiral N droplets did depend on the size of the droplets: the bigger

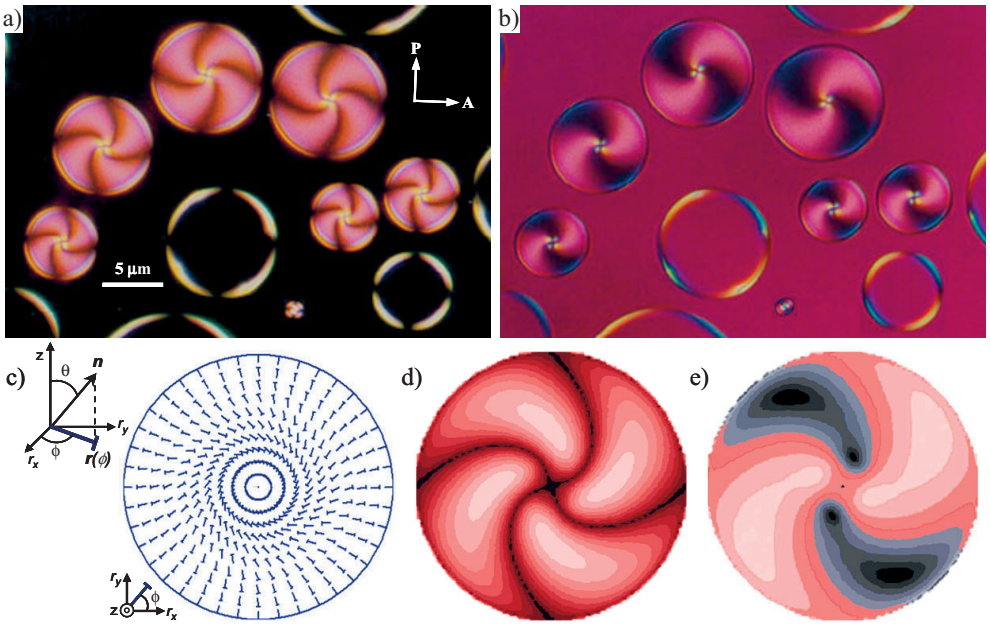

Figure 3. Propeller-patterned chiral N POM textures of BPCA-C7-P*m*OH in a bare glass cell: POM textures a) without and b) with a tint-retardation plate (530 nm) between the analyzer and the sample at 216 °C. c) Computer-simulated molecular-packing model in a right-handed propeller-patterned N droplet. Here, *n* is the LC molecular director with the twist angle (θ) from the cylinder axis (*z*), $r(\phi)$ is the projection of *n* on the $r_x r_y$ plane, and ϕ is the azimuthal twist angle. Calculated optical textures based on the molecular arrangement in (c) under POM d) without and e) with a tint-retardation plate between the analyzer and the sample.

droplets possessed longer pitch lengths. Since the sizes of the propeller-patterned chiral N droplets were almost identical to those of the achiral N droplets, the chiral propeller-shaped N droplets should not have developed due to the confinement effect of the achiral molecules.[31,32] Furthermore, when two propeller-patterned chiral N droplets with identical handedness merged, a bigger chiral propeller-patterned N droplet with the same handedness was formed (Fig. 4a). On the other hand, if two propeller-patterned chiral N droplets with opposite handedness merged, an achiral N droplet was formed (Fig. 4b). Therefore, achiral N droplets may be formed from a racemic mixture of both right-handed and left-handed twisted chiral conformers, and chiral propeller-patterned N droplets may be formed from twisted chiral conformers, even though their pitch lengths depend on the size of N droplets.

In summary, a series of achiral BPCA-C*n*-P*m*OHs exhibited chiral cholesteric behavior in an N phase. The origin of the chiral N phases in these achiral molecules came from the twisted conformation of individual head-to-head dimers, indicating for the first time that neither molecular chirality nor a molecular bend is necessary to form a chiral phase. Different chiral N architectures were observed, depending on the substrate surface chemistry. A Frank–Pryce spherulitic N droplet with equidistant rings, and fingerprint textures with equidistant lines of these achiral molecules resulted from the single-twisting of chiral conformers; while the observed propeller-patterned chiral N droplets were formed by the double-twisting of chiral conformers in the chiral N phase. In addition to the insight into the fundamental physics of chiral phases, this series of molecules can also be used as an intermediary to recognize the chiral molecules that are often observed in configurational chiral molecular systems.[1–7]

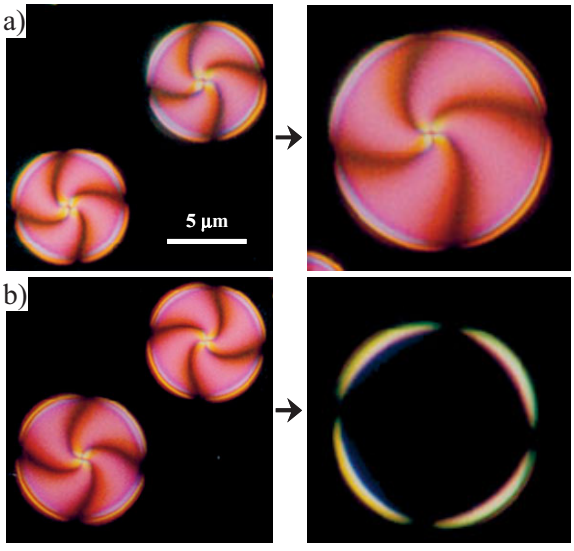

Figure 4. Propeller-patterned chiral N POM textures of the BPCA-C7-P*m*OH sample in a bare glass cell: a) two left-handed N droplets merged into a bigger left-handed N droplet and b) a right-handed and a left-handed N droplet merged into a bigger achiral N droplet.

ADVANCED MATERIALS

Experimental

Materials and Sample Preparations: A series of achiral BPCA-C*n*-P*m*OH molecules ($n = 6$–10) were synthesized using four-step substitution reactions [24]. For the DSC experiments, the sample mass was 2 mg and the pan masses were kept constant with a precision of ±0.001 mg. The sample thickness for POM was 5 μm, and samples were melt-processed between two polyimide-coated/rubbed glass substrates [26] or between two bare glass substrates that were cleaned with a HCl/water solution.

Equipment and Experiments: The thermal transitions were studied using a Perkin–Elmer PYRIS Diamond DSC with an Intracooler 2P apparatus. The temperatures and heat flows were calibrated using benzoic acid and indium at different cooling and heating rates. Overlapped transition peaks were resolved using the PeakFit deconvolution program. Asymmetric Gaussian and Lorentzian functions were used to obtain the best fit. The WAXD patterns were obtained using a Rigaku X-ray imaging system with an 18 kW rotating anode X-ray generator. Additionally, a hot stage was used to measure LC structures at elevated temperatures. The optical textures of the LC phases at different temperatures were observed with a POM (Olympus BH-2) coupled with a Mettler heating stage (FP-90). The temperature of this hot stage was calibrated to be within ±0.5 °C. A tint-retardation plate (530 nm), between the sample and the analyzer, was used to study the molecular orientation in the N droplets. The contact angles of the glass substrates were measured with a 10 mL water drop using a Rame Hart NRL-100. Cerius^2 (Version 4.6) software from Accelrys was used to calculate the head-to-head dimer minimal energy geometry of BPCA-C*n*-P*m*OH in the isolated gas-phase, utilizing the COMPASS force field. The Oseen–Frank elastic-energy-density free energy was used to calculate the molecular-packing model in the propeller-patterned chiral N droplet. The helical pitch (P) was $2R$ (R is radius of droplet), the extraordinary refractive index (n_e) was 1.6, and the ordinary refractive index (n_o) was 1.5. In order to minimize the Oseen–Frank elastic-energy-density free energy, we used the approximation of K_{11} (splay elastic constant) = K_{33} (bend elastic constant) = $3.333K_{22}$ (twist elastic constant), without a loss of generality.

Received: June 15, 2006
Revised: September 5, 2006

[1] J. W. Goodby, in *Handbook of Liquid Crystals*, Vol. 1 (Eds: D. Demus, J. Goodby, G. W. Gray, H.-W. Spiess, V. Vill), Wiley-VCH, Weinheim, Germany **1998**, p. 115.
[2] H.-S. Kitzerow, C. Bahr, in *Chirality in Liquid Crystals* (Eds: H.-S. Kitzerow, C. Bahr), Springer, London **2001**, p. 1.
[3] J. H. K. K. Hirschberg, L. Brunsveld, A. Ramzi, J. A. J. M. Vekemans, R. P. Sijbesma, E. W. Meijer, *Nature* **2000**, *407*, 167.
[4] A. Y. Bobrovsky, N. I. Boiko, V. P. Shibaev, J. Springer, *Adv. Mater.* **2000**, *12*, 1180.
[5] T. Kato, N. Mizoshita, K. Kanie, *Macromol. Rapid Commun.* **2001**, *22*, 797.
[6] D. N. Reinhoudt, M. Crego-Calama, *Science* **2002**, *295*, 2403.
[7] P. Z. Guo, L. Zhang, M. H. Liu, *Adv. Mater.* **2006**, *18*, 177.
[8] S. F. Mason, *Nature* **1984**, *311*, 19.
[9] J. W. Goodby, *Science* **1986**, *231*, 350.
[10] C. Y. Li, S. Z. D. Cheng, J. J. Ge, F. Bai, J. Z. Zhang, I. K. Mann, L. C. Chien, F. W. Harris, B. Lotz, *J. Am. Chem. Soc.* **2000**, *122*, 72.
[11] C. Y. Li, S. Z. D. Cheng, X. Weng, J. J. Ge, F. Bai, J. Z. Zhang, B. H. Calhoun, F. W. Harris, L. C. Chien, B. Lotz, *J. Am. Chem. Soc.* **2001**, *123*, 2462.
[12] H. Finkelmann, S. T. Kim, A. Muñoz, P. Palffy-Muhoray, B. Taheri, *Adv. Mater.* **2001**, *13*, 1069.
[13] R. Purrello, *Nat. Mater.* **2003**, *2*, 216.
[14] T. Yoshioka, T. Ogata, T. Nonaka, M. Moritsugu, S.-N. Kim, S. Kurihara, *Adv. Mater.* **2005**, *17*, 1226.
[15] J. M. Gao, H. B. Liu, E. T. Kool, *Angew. Chem. Int. Ed.* **2005**, *44*, 3118.
[16] S. Furumi, Y. Sakka, *Adv. Mater.* **2006**, *18*, 775.
[17] T. R. Linderoth, *Nat. Mater.* **2006**, *5*, 112.
[18] T. Niori, T. Sekine, J. Watanabe, T. Furukawa, H. Takezoe, *J. Mater. Chem.* **1996**, *6*, 1231.
[19] D. R. Link, G. Natale, R. Shao, J. E. MacLennan, N. A. Clark, E. Korblova, D. M. Walba, *Science* **1997**, *278*, 1924.
[20] G. Pelzl, S. Diele, A. Jákli, C. Lischka, I. Wirth, W. Weissflog, *Liq. Cryst.* **1999**, *26*, 135.
[21] J. Thisayukta, H. Niwano, H. Takezoe, J. Watanabe, *J. Am. Chem. Soc.* **2002**, *124*, 3354.
[22] M. Gimeno, M. B. Ros, J. L. Serrano, M. R. de la Fuente, *Angew. Chem. Int. Ed.* **2004**, *43*, 5235.
[23] T. Kajitani, H. Masu, S. Kohmoto, M. Yamamoto, K. Yamaguchi, K. Kishikawa, *J. Am. Chem. Soc.* **2005**, *127*, 1124.
[24] K. U. Jeong, S. Jin, J. J. Ge, B. S. Knapp, M. J. Graham, J. J. Ruan, M. M. Guo, H. Xiong, F. W. Harris, S. Z. D. Cheng, *Chem. Mater.* **2005**, *17*, 2852.
[25] K. U. Jeong, B. S. Knapp, J. J. Ge, S. Jin, M. J. Graham, F. W. Harris, S. Z. D. Cheng, *Chem. Mater.* **2006**, *18*, 680.
[26] J. J. Ge, G. Xue, C. Y. Li, I. K. Man, W. Zhou, S.-Y. Wang, F. W. Harris, S. Z. D. Cheng, S.-C. Hong, X. Zhuang, Y. R. Shen, *J. Am. Chem. Soc.* **2001**, *123*, 5768.
[27] I. Dierking, *Texture of Liquid Crystals*, Wiley-VCH, Weinheim, Germany **2003**.
[28] R. R. Swisher, H. Huo, P. P. Crooker, *Liq. Cryst.* **1999**, *26*, 57.
[29] H.-S. Kitzerow, in *Liquid Crystals in Complex Geometries* (Eds: G. P. Crawford, S. Zumer), Taylor and Francis, London **1996**, p. 187.
[30] N. Murazawa, S. Juodkazis, S. Matsuo, H. Misawa, *Small* **2005**, *1*, 656.
[31] Y. T. Tao, M. T. Lee, S. C. Chang, *J. Am. Chem. Soc.* **1993**, *115*, 9547.
[32] R. Arnold, W. Azzam, A. Terfort, C. Wöll, *Langmuir* **2002**, *18*, 3980.

